Bulgarian Chemical Communications, Volume 49, Special Issue G (pp.217 –224) 2017

Studies of the possibilities to obtain nanosized $MnFe_2O_4$ by solution combustion synthesis

Ts. Lazarova[1]*, D. Kovacheva[1], Z. Cherkezova-Zheleva[2], G. Tyuliev[2]

[1]*Institute of General and Inorganic Chemistry, Bulgarian Academy of Sciences, Acad. G. Bonchev str., Bl 11, Sofia-1113, Bulgaria,*

[2]*Institute of Catalysis, Bulgarian Academy of Sciences, Acad. G. Bonchev str., Bl 11, Sofia-1113, Bulgaria*

Received November 10, 2016; Revised January 3, 2017

Nanosized $MnFe_2O_4$ has important applications such as magnetic recording devices, ferrofluids, biosensors, catalysts, guided transport and delivery of drugs in the body and others. The possibilities to obtain nanosized $MnFe_2O_4$ using the method of solution combustion synthesis are studied in this work. Two systems with mixed fuels in various ratios, namely glycine-glycerol and sucrose-urea are studied. The obtained products are thermally treated at various temperatures and in various atmospheres (air, argon) to find optimal conditions for obtaining single phase nano-sized $MnFe_2O_4$. Samples were studied by the methods of X-ray diffraction (XRD), X-ray photoelectron spectroscopy (XPS), low-temperature nitrogen adsorption (BET), and Mössbauer spectroscopy. Samples obtained by using pure hydrocarbons or mixtures with high content of hydrocarbons show superparamagnetic behavior due to the small size of the crystallites while samples obtained with high content of nitrogen containing fuels show magnetic ordering**.** It was shown that smaller particles obtained at low temperatures of thermal treatment demonstrate higher strain. Thermal treatment at higher temperatures leads to decrease of the strain without significant change of the size of the crystallites.

Keywords: *solution combustion synthesis, $MnFe_2O_4$, XRD, XPS, Mössbauer spectroscopy*

INTRODUCTION

Nanoscale and nanostructured materials are among the most important priorities of modern materials science. In recent years, various technological applications based on nano-sized ferrite materials were developed using of their unique magnetic, electrical and optical properties. An important representative of the ferrite family is $MnFe_2O_4$. It is well known that it is partially inverse spinel, in which about 20% of Mn^{2+} ions occupy octahedral sites (B) and 80% of them are located in tetrahedra (A). Cation distribution in spinels is very important and directly affects its physical properties [1, 2]. In recent years nano-sized $MnFe_2O_4$ has received increasing research interest because of its remarkable magnetic properties (low coercivity, moderate magnetization) combined with good chemical resistance, high permeability and mechanical strength [3]. The high density of $MnFe_2O_4$ underlies its technological applications as core materials for coils, transformers, information and communication devices and others [4]. Nanoscale $MnFe_2O_4$ is interesting for other practical applications, namely as contrast agent for magnetic resonance imaging, magnetic drug delivery for cancer treatment by hyperthermia and others [5 - 7]. Another important application of nano-sized $MnFe_2O_4$ in the last decade is the removal of heavy metals and a variety of toxic organic pollutants from waste water [8, 9]. The use of nano-sized manganese ferrite as a sensor for monitoring the environment is based on its high specific surface area. The same fact lies at the basis of the use of this material as a catalyst [10, 11] and as electrode material in asymmetric supercapacitors [12, 13]. Physical and chemical properties of $MnFe_2O_4$ are strongly dependent on its structural and micro-structural characteristics that are directly related to and can be controlled during the synthesis process [14]. Various methods for preparing nano-sized $MnFe_2O_4$ have been developed, such as sol-gel [15], co-precipitation [16], hydrothermal method [17], solid state reaction [18, 19], thermal decomposition [20], solution combustion synthesis [21, 22], mechanochemical reaction [23], etc. Among them solution combustion synthesis is considered as very appropriate for preparation of nano-sized materials due to the fact that this method is simple, fast, versatile, and cost-effective [24]. In our previous study concerning the preparation of nano-sized $NiFe_2O_4$ using the solution

* To whom all correspondence should be sent.
E-mail: cveti_ura@abv.bg

combustion method was found that the type of the fuel component has an influence both on structural characteristics (cation distribution) and on the morphological characteristics (size and shape of the particles, aggregation ability, etc.) [25]. The aim of this work was to study the influence of mixing of different types of fuel (nitrogen-containing and hydrocarbons) at different ratios in the systems of fuels: sucrose-urea and glycine-glycerol for preparing a single phase $MnFe_2O_4$ and to study the influence of mixing of different types of fuels on structural and morphological characteristics of the obtained powders.

MATERIALS AND METHODS

The method of solution combustion synthesis was used to obtain nano-sized $MnFe_2O_4$. Metal nitrates (oxidizers) and fuels sucrose, urea, glycine, and glycerol in various ratios were used. The ratio of the amounts of oxidant and fuel was based on the proposed by Jain *et al* theory [26]. Stoichiometric amounts of the starting reagents were dissolved in an appropriate amount of deionized water. The resulting solutions were heated on a magnetic stirrer. Initially, the solution was dehydrated, and then the residue reaches its point of ignition and ignites. The obtained powders were then thermally treated at various temperatures from 400 to 700ºC for one hour in a different atmosphere (air, argon). Structural characteristics of all samples were studied with powder X-ray diffractometer Bruker D8 Advance with Cu-Kα radiation and LynxEye detector. Powder diffraction patterns were collected in the range from 10 to 90 deg. 2θ with a step 0.03 deg. 2θ rotating the sample with 15 rpm. Phase analysis was performed with the software package Diffracplus EVA using the database ICDD-PDF2 (2014). The unit cell parameters and mean crystallite sizes were determined with the program Topas - 4.2 [27]. The specific surface areas (SSA) was determined by low temperature nitrogen adsorption (BET) method in an equipment Quantachrome Instruments NOVA 1200e (USA). The particle size and morphology were studied by a transmission electron microscopy (TEM) with a TEM JEOL 2100 at 200 kV. The XPS measurements were carried out in the analysis chamber of the electron spectrometer Escalab-MkII (VG Scientific) with a base pressure of ~5 x 10^{-8} Pa. The C1s, O1s, Mn2p, Fe2p and Mn3s photoelectron lines were evaluated by using the normalized photoelectron intensities [28]. Mössbauer spectra were recorded on electromechanical spectrometer (Wissenschaftliche Elektronik GMBN, Germany) operating under constant acceleration at room temperature. As a source 57Co/Cr was used (Activity >50 mCi). The standard material was α-Fe. The spectra were processed using a program based on the least squares method.

RESULTS AND DISCUSSION

The possibilities for obtaining nano-sized $MnFe_2O_4$ were studied when as a fuel were used mixture of sucrose-urea or glycin-glycerol in various ratios, namely: 1:0, 0.75:0.25; 0.5:0.5, 0.25:0.75 and 0:1. All samples were thermally treated for one hour at a temperature ranging between 400 and 700ºC in air and in argon atmosphere. The obtained materials were analyzed by powder X-Ray diffraction. Table 1 and Table 2 show the results for phase composition of these samples. As can be seen from Table 1 single-phase product was obtained when using only sucrose as a fuel and for the sucrose-urea fuel mixtures, for fuel compositions with higher sucrose content. Preparation of single-phase product using urea as a fuel was not observed. In the second fuel system, the formation of single phase nano-sized $MnFe_2O_4$ was observed when using glycerol as fuel and for fuel compositions with higher glycerol content. Formation of single phase $MnFe_2O_4$ using only glycine as a fuel was not observed. In all the samples thermally treated at a temperatures above 600ºC in both atmospheres (air, argon) a decomposition of the spinel phase to the individual oxides (Fe_2O_3-hematite and Mn_2O_3-bixbite) was observed. It deserves commenting that samples prepared with high content of nitrogen-containing fuels show impurity phase of oxides of divalent ions (Fe^{2+}, Mn^{2+}) which indicates that synthesis reaction proceeds at high temperatures and with the release of gases that promote the reduction of metal ions. These observations leads to the conclusion that single-phase nano-sized $MnFe_2O_4$ can be synthesized using either pure hydrocarbons (sucrose, glycerol) as a fuel or having fuel mixtures with high content of hydrocarbons.

From the data presented in Table 1 and Table 2 it may be concluded that single phase spinel product can be obtained at temperatures below 600ºC from fuel mixtures containing high content of hydrocarbons. In Fig. 1 (a-d) are presented powder diffraction patterns of some $MnFe_2O_4$ synthesized using a mixture of fuels (a, b) sucrose-urea, (c, d) glycine-glycerol. All diffraction lines can be indexed within the cubic Space group Fd-3m.

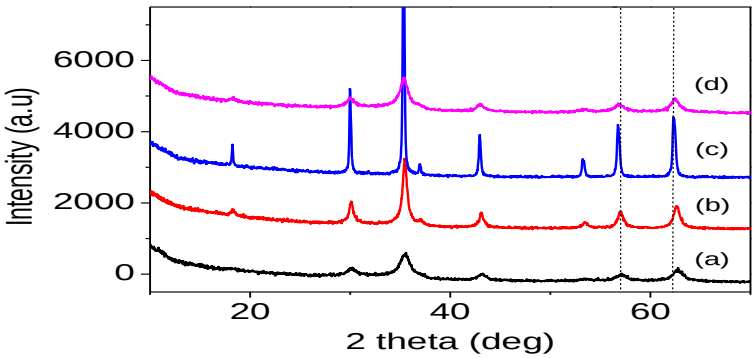

Fig. 1. XRD patterns of nanosized $MnFe_2O_4$ synthesized by (a) sucrose-urea 0.75:0.25 at 500°C, (b) sucrose-urea 0.25: 0.75 at 500°C, (c) glycine-glycerol 0.75: 0.25 at 400°C (Ar) and (d) glycine-glycerol 0.25:0.75 at 500°C (Ar).

Table 1. Phase composition of samples synthesized with mixture of sucrose and urea at different ratios, thermally treated at 400 to 700°C in Air and Argon atmosphere. Identified phases were manganese ferrite spinel-$MnFe_2O_4$, bixbite-Mn_2O_3, hematite-Fe_2O_3 and wustite (Fe,Mn)O.

Air		Argon	
Fuel/Temperature	Identified phases	Fuel/Temperature	Identified phases
sucrose		***sucrose***	
400°C	**spinel**	400°C	**spinel**
500 °C	**spinel**	500 °C	**spinel**
600 °C	bixbite + hematite	600 °C	spinel +wustite
700 °C	bixbite + hematite	700 °C	spinel +wustite
sucrose and urea 0.75:0.25		***sucrose and urea 0.75:0.25***	
400 °C	**spinel**	400 °C	**spinel**
500 °C	**spinel**	500 °C	**spinel**
600 °C	bixbite + hematite	600 °C	spinel + bixbite +hematite
700 °C	bixbite + hematite	700 °C	Traces of spinel + bixbite + hematite
sucrose and urea 0.5:0.5		***sucrose and urea 0.5:0.5***	
400 °C	**spinel**	400 °C	**spinel**
500 °C	**spinel**	500 °C	**spinel**
600 °C	bixbite + hematite	600 °C	spinel + hematite
700 °C	bixbite + hematite	700 °C	spinel + bixbite + hematite
sucrose and urea 0.25:0.75		***sucrose and urea 0.25:0.75***	
400 °C	**spinel**	400 °C	**spinel**
500 °C	**spinel**	500 °C	**spinel**
600 °C	bixbite + hematite	600 °C	traces of spinel + hematite
700 °C	bixbite + hematite	700 °C	traces of spinel + bixbite + hematite
urea		***urea***	
400 °C	spinel + bixbite	400 °C	**spinel**
500 °C	spinel + bixbite + hematite	500 °C	spinel + hematite
600 °C	bixbite + hematite	600 °C	spinel + hematite
700 °C	bixbite + hematite	700 °C	spinel + hematite

Table 2. Phase composition of samples synthesized with mixture of glycine and glycerol at different ratios, thermally treated at 400 to 700°C in Air and Argon atmosphere. Identified phases were manganese ferrite spinel-$MnFe_2O_4$, bixbite-Mn_2O_3, hematite-Fe_2O_3 and wustite (Fe,Mn)O.

Air		Argon	
Fuel/Temperature	Identified phases	Fuel/Temperature	Identified phases
glycine		***glycine***	
400ºC	spinel + wustite	400ºC	spinel + wustite
500 ºC	traces of spinel+ bixbite+ hematite	500 ºC	spinel +wustite
600 ºC	traces of spinel +bixbite + hematite	600 ºC	spinel + hematite
700 ºC	bixbite + hematite	700 ºC	spinel + hematite
glycine and glycerol 0.75:0.25		***glycine and glycerol 0.75:0.25***	
400 ºC	three unknoun spinels	400 ºC	**spinel**
500 ºC	three unknoun spinels	500 ºC	spinel+ hematite + maghemite
600 ºC	bixbite + hematite	600 ºC	traces of spinel+ bixbite + hematite
700 ºC	bixbite + hematite	700 ºC	traces of spinel +bixbite + hematite
glycine and glycerol 0.5:0.5		***glycine and glycerol 0.5:0.5***	
400 ºC	**spinel**	400 ºC	**spinel**
500 ºC	**spinel**	500 ºC	spinel + hematite
600 ºC	bixbite + hematite	600 ºC	traces of spinel+ bixbite + hematite
700 ºC	bixbite + hematite	700 ºC	traces of spinel bixbite + hematite
glycine and glycerol 0.25:0.75		***glycine and glycerol 0.25:0.75***	
400 ºC	**spinel**	400 ºC	**spinel**
500 ºC	**spinel**	500 ºC	**spinel**
600 ºC	bixbite + hematite	600 ºC	traces of spinel+ bixbite + hematite
700 ºC	bixbite + hematite	700 ºC	traces of spinel+ bixbite + hematite
glycerol		***glycerol***	
400 ºC	**spinel**	400 ºC	**spinel**
500 ºC	spinel + traces of hematite	500 ºC	**spinel**
600 ºC	bixbite + hematite	600 ºC	traces of spinel+ bixbite + hematite
700 ºC	bixbite + hematite	700 ºC	traces of spinel + bixbite + hematite

Diffraction patterns indicate the formation of single-phase spinels, but also reveal that materials, obtained with different fuel mixture differ strongly by their mean crystallite size and unit cell parameters. This fact indicates that the mixture of fuels produces different synthesis conditions thus leading to the production of materials with different structural and morphological characteristics.

A significant difference in particles morphology can be seen from the TEM-photographs of the materials synthesized with the use of different fuel mixtures. Fig. 2 represents the TEM images of $MnFe_2O_4$ synthesized using a mixture of sucrose-urea (a, b) and glycine-glycerol (c, d) fuels. TEM images show poorly shaped particles with an average size smaller than 10 nm for the materials obtained with the use fuel mixture of sucrose-urea and glycine-glycerol with high hydrocarbons content. The exception is the sample from glycine-glycerol fuel system with high content of glycine (Fig. 2c), where the average size is about 50 nm.

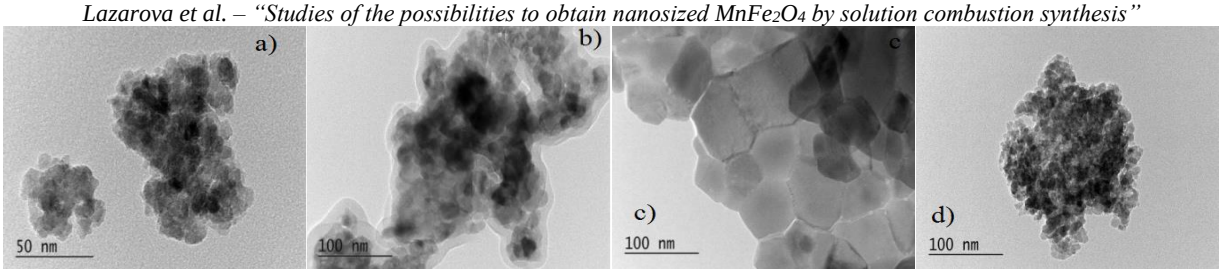

Fig. 2. TEM image of nano-sized $MnFe_2O_4$ synthesized by using a mixture of fuels: (a) sucrose-urea 0.75:0.25 at 500°C, (b) sucrose-urea 0.25: 0.75 at 500°C, (c) glycine-glycerol 0.75: 0.25 at 400°C (Ar) and (d) glycine-glycerol 0.25:0.75 at 500°C (Ar).

Table 3. Structural parameters determined by XRD analysis of nano-sized $MnFe_2O_4$ synthesized by using mixture of sucrose and urea fuels in different ratio and thermally treated in Air or Argon atmosphere.

fuel	temperature °C	unit cell parameter (Å)	mean crystallite size, nm	SSA,m^2/g / mean size derived from BET, nm	Strain $x10^{-4}$
sucrose	400 °C	8.35	5.7		69.17
	500 °C	8.34	6.4	88/12.7	56.82
sucrose and urea 0.75:0,25	400 °C	8.35	6.9		52.46
	500 °C	8.379	19.1	85/13.15	13.96
sucrose and urea 0,5:0,5	400°C	8.38	15.8	44 /25.4	18.94
	500°C	8.379	20.04	39/28.66	16.32
sucrose and urea 0.25:0.75	400°C	8.38	20.57		17.99
	500°C	8.352	6.6	40/27.9	44.92
sucrose (Argon)	400°C	8.439	5.9	85/13.15	51.39
	500°C	8.5142	14.2	44/25.4	25.76
sucrose and urea 0.75:0.25 (Argon)	400°C	8.387	6.8		44.83
	500°C	8.401	7.8	98/11.5	37.07
sucrose and urea 0.5:0.5 (Argon)	400°C	8.500	13.3		15.06
	500°C	8.499	26.1	54/20.7	33.97
sucrose and urea 0.25:0.75 (Argon)	400°C	8.456	7.2		30.7
	500°C	8.461	6.8	82/13.63	61.3

Table 4. Structural parameters determined by XRD analysis of nanosized $MnFe_2O_4$ synthesized by using mixture of glycine and glycerol fuels in different ratio and thermally treated in air or argon atmosphere.

fuel	temperature °C	unit cell parameter Å	mean crystallite size, nm	SSA,m^2/g / mean size derived from BET, nm	Strain $x10^{-4}$
glycine and glycerol 0.5:0.5	400 °C	8.37	11		19.33
	500 °C	8.38	12		11.44
glycine and glycerol 0.25:0.75	400 °C	8.37	12		8.06
	500 °C	8.38	15	60 /18.63	7.85
glycerol	400°C	8.37	11		13.03
glycine and glycerol 0.75:0.25 (Argon)	400°C	8.4208	59	11/102	6.04
glycine and glycerol 0.5:0.5 (Argon)	400°C	8.38	10		36.19
glycine and glycerol 0.25:0.75 (Argon)	400°C	8.45	9.7	96/11.64	37.42
	500°C	8.41	10.4	86/13	11.52
Glycerol (Argon)	400°C	8.44	13		45.32
	500°C	8.40	13		13.05

Table 3 and Table 4 show the unit cell parameters, mean coherent domain sizes and microstrains for all single-phase samples, and for some of them the specific surface areas. Samples obtained from both fuel systems and thermally treated in argon atmosphere show spinel phase with higher unit cell parameters and higher specific surface areas than those thermally treated in air atmosphere. At the same time the mean crystallite domain sizes of the samples treated in different atmospheres show similar values.

The data presented in Table 3 and Table 4 show correlation between unit cell parameters, mean crystallite sizes and residual microstrains. In general, samples with small unit cell parameters have also small mean crystallite size and high values of lattice strain. Thermal treatment at higher temperatures leads to decrease of the strain without significant change of the size of the crystallites. The differences in unit cell parameters can be due to differences of oxidation state of cations, as well as to different cation distributions into two cation sublattices in the spinel structure (tetrahedral and octahedral).

The Mn2p and Fe2p photoelectron lines are shown on Fig. 3. The $Mn2p_{3/2}$ binding energy value of 642.0 eV is slightly higher than expected for Mn^{2+} i.e. 641.3 eV [29, 30]. In addition, the absence of satellite at ~ 647 eV is an indication for the possible presence of Mn in oxidation state higher than 2+ due to air exposure after samples preparation. The $Fe2p_{3/2}$ main line has maximum at 711.0 eV, a value characteristic of Fe^{3+} as in Fe_2O_3 [31].

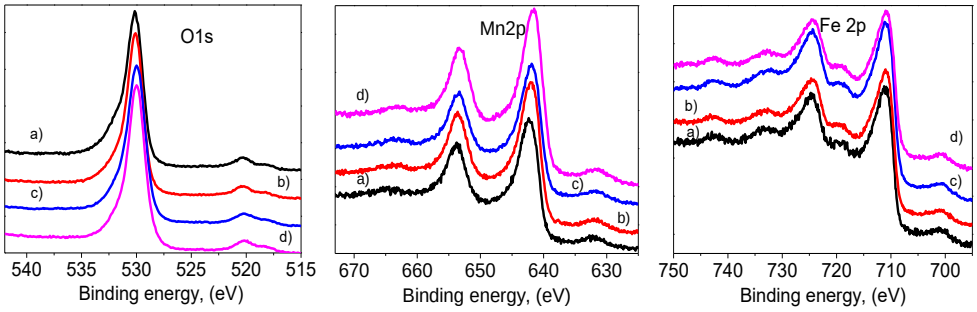

Fig. 3. O1s, Mn2p and Fe2p photoelectron lines for $MnFe_2O_4$ samples synthesized by (a) sucrose-urea 0.75:0.25 at 500°C, (b) sucrose-urea 0.25: 0.75 at 500°C, (c) glycine-glycerol 0.75: 0.25 at 400°C (Ar) and (d) glycine-glycerol 0.25:0.75 at 500°C (Ar).

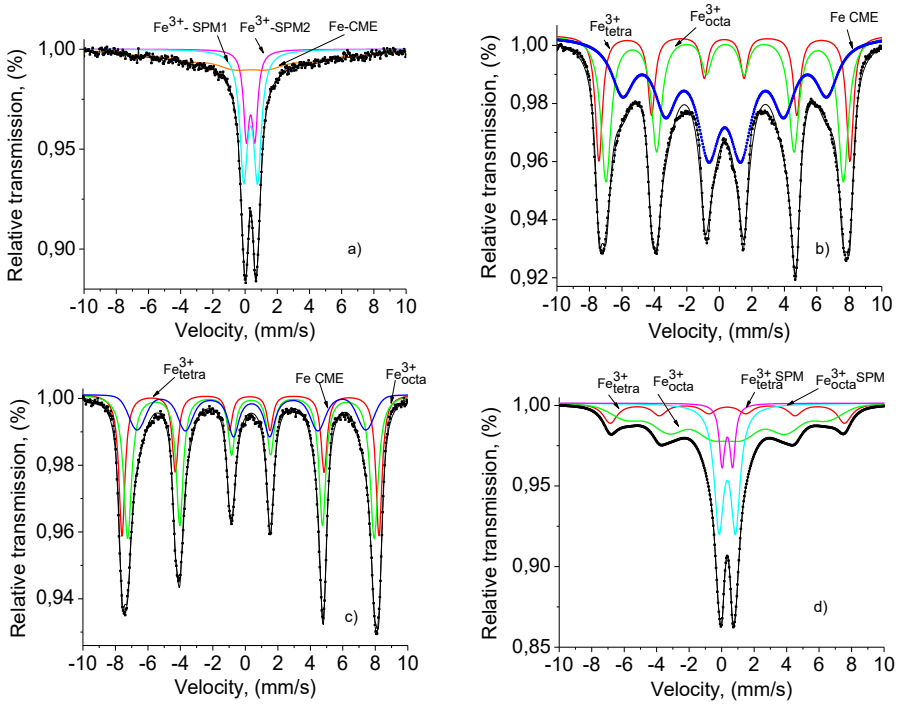

Fig. 4. The Mössbauer spectra of $MnFe_2O_4$ synthesized by (a) sucrose at 500°C (Ar), (b) sucrose-urea 0.5:0.5 at 500°C, (c) glycine-glycerol 0.75: 0.25 at 400°C (Ar) and (d) glycine-glycerol 0.25:0.75 at 500°C (Ar).

The Fe^{3+} ions can be distinguished also by the small satellite appearing at higher binding (~8.5 eV above the main line). The position of O1s peak practically does not change for all samples and has a binding energy of 530.0 eV, a value typical for lattice oxygen in transition metal oxides. The higher binding energy shoulder is usually assigned to species adsorbed on surface defect structures, OH group and/or adsorbed water.

The Mössbauer spectra at room temperature of some of synthesized samples are shown on Fig. 4. It can be seen that all the experimental spectra are complicated and include unresolved components. Two of materials, $MnFe_2O_4$ synthesized by sucrose-urea 0.5:0.5 and glycine-glycerol 0.75:0.25 (Ar), have only sextet components i.e. magnetic structure. The spectra of $MnFe_2O_4$ synthesized by sucrose (Ar) and glycine-glycerol 0.25:0.75 (Ar), contain both doublet and sextet components. The calculated hyperfine parameters IS and QS suggest the presence of spinel ferrite material with critically small particle size. This leads to registration of relaxation effects as superparamagnetism (SPM) and collective magnetic excitation behavior (CME) [32, 33].

CONCLUSION

Single phase nanosized spinel manganese ferrites were prepared by solution combustion method using two mixtures of fuels urea-sucrose and glycine-glycerol in different ratios. The type of fuel has a strong influence on the possibilities to obtain single-phase product. The analyses indicate that single-phase product was obtained using pure hydrocarbons as fuel or fuel mixtures with high content of hydrocarbons. The spinel phase decomposes to individual oxides at temperatures above 600°C despite the atmosphere of thermal treatment. Samples obtained by using pure hydrocarbons or mixtures with high content of hydrocarbons show superparamagnetic behaviour due to the small size of the crystallites while samples obtained with high content of nitrogen containing fuels show magnetic ordering**.** It was shown that smaller particles obtained at low temperatures of thermal treatment demonstrate higher strain. Thermal treatment at higher temperatures leads to decrease of the strain without significant change of the size of the crystallites.

Acknowledgment*: This work is performed with the financial support of the Program for career development of young scientists, BAS and National Science Fund of Bulgaria under the contract DFNI E02/18.*

REFERENCES

1. M.Y. Rafique, P.L.Qing, Q. Javed, M.Z. Iqba, Q.H. Mei, M.H. Farooq, G.Z.Gang, M. Tanveer, *Chin. Phys.* B **22** (10), 107101 (2013).
2. N.M. Deraz, A. Alarifi,. *Int. J. Electrochem. Sci*. **7**, 5534 (2012).
3. A. Goldman, *Modern Ferrite Technology*, Marcel Dekker, New York 54**,** (1993).
4. D. Shi, B. Aktas, L.Pust, F. Mikailov, *Nanostructured Magnetic Materials and Their Applications* **593,** (2002).
5. S. Seifikar, B. Calandro, E. Deeb et al., *Journal of Applied Physics* **112,** 12391 (2012).
6. S. Seifikar, A. Tabei, E. Sachet et al., *Journal of Applied Physics* **112,** 063908, (2012).
7. S. Shafiu, R. Topkaya, A. Baykal, M.S. Toprak, *Materials Research Bulletin* **48,** 4066 (2013).
8. L. X. Yang, F. Wang, Y. F. Meng, Q. H . Tang, Z. Q. Liu, *J . Nanomater,* 263 (2013).
9. N. Mahmoodi, *J Environ Eng*. **139** (11), 1382 (2013).
10. N. M. Mahmoodi, M. Arabloo, J. Abdi, *Water Res*. **67**, 216 (2014).
11. T. V. Solis, P. Tartaj, G. Marban, A. B. Fuertes, *Catal Commun* **8**, 2037 (2007).
12. S. L. Kuo, N. L. Wu, *Electrochem. Solid-State Lett.* **8**, A495 (2005).
13. S. L. Kuo, J. F. Lee, N. L. Wu, *J. Electrochem. Soc.* **154**, A34 (2007).
14. J. Wang, Q. Chen, B. Hou, Z.Peng, *J. Inorg Chem*. **6**, 1165 (2004).
15. L. Jianjun, Y. Hongming, L. Guodong, L. Yanju, L. Jinsong, *J. Magn. Magn Mater* **322** , 3396 (2010).
16. J. Amighian, M. Mozaffari, B. Nasr, *Phys. Status Solidi* C**3**, 3188 (2006).
17. P. A. Seema Verma, Y. B. Joy, H. S. Khollam, S.B. Potdar, *Mater.Lett*. **58**, 1092 (2004).
18. H. H. Kedesdy, A. Tauber, *J Am Ceram Soc*. **39**, 425 (1956).
19. T. K. Kundu, S. Mishra, *Bull Mater Sci*. **31**, 507 (2008).
20. H. Yang, C. Zhang, X. Shi, H. Hu, X. Du, Y. Fang, Y. Ma, H. Wu, S. Yang, *Biomaterials* **31**, 3667 (2010).
21. K. Suresh, N. R. S. Kumar, K. C. Patil, *Adv. Mater.* **3**, 148 (1991).
22. S. Sam, A. Samson Nesaraj, *International Journal of Applied Science and Engineering* **9**, (4) 223 (2011).
23. P. Osmokrovi, C. Jovaleki, D. Manojlovi, M. B. Pavlovi, *Journal of optoelectronics and advanced materials* **8**, 312 (2006).
24. K.C. Patil, S. T.Aruna, S. Ekambaram, *Solid State &Materials Science* **2**, 158 (1997).
25. Ts. Lazarova, M. Georgieva, D. Tzankov, D. Voykova, L. Aleksandrov, Z. Cherkezova-

Zheleva, D. Kovacheva, *Journal of Alloys and Compounds*, in press.
26. S. R. Jain, K. C. Adiga, V. R Pai Verenekar, *Combustion and Flame* **40**, 71 (1981).
27. Bruker TOPAS, Version 4.2, Bruker AXS, Karlsruhe, Germany (2007).
28. J. H. Scofield, *Journal of electron spectroscopy and related phenomena* **8**, (2) 129 (1976).
29. M. A. Langell, C. W. Hutchings, G. A. Carson, M. H. Nassir, *J. Vac. Sci. Technol*. **A 14**, 1656 (1996).
30. D. Kovacheva, T. Trendafilova, K. Petrov A. Hewat, *Journal of Solid State Chemistry*, **169**, 44 (2002).
31. T. Yamashita, P. Hayes, *Applied Surface Science* **254**, 2441 (2008).
32. F. L. Deepak, M. Bañobre-López, E. Carbo-Argibay, M. Cerqueira, Y. Piñeiro-Redondo, J. Rivas, C. M. Thompson, S. Kamali, C. Rodriguez-Abreu, K. Kovnir, Y. V. Kolen'ko, *J. Phys. Chem. C* **119,** (21) 11947 (2015).
33. A. Yang, C. N. Chinnasamy, J. M. Greneche, Y. Chen, S. D. Yoon, Z.i Chen, K. Hsu, Z. Cai, K. Ziemer, C. Vittoria, V. G. Harris, *Nanotechnology* **20,** 185704 (2009).

ИЗСЛЕДВАНЕ НА ВЪЗМОЖНОСТИТЕ ЗА ПОЛУЧАВАНЕ НА НАНОРАЗМЕРЕН $MnFe_2O_4$ ПРИ СИНТЕЗ ПО МЕТОДА НА ИЗГАРЯНЕ ОТ РАЗТВОР

Цв. Лазарова[1], Д. Ковачева[1], З. Черкезова-Желева[2], Г. Тюлиев[2]

[1]Институт по обща и неорганична химия, Българска академия на науките, ул. акад. Г. Бончев, Бл 11, София-1113, България, cveti_ura@abv.bg
[2]Институт по катализ, Българска академия на науките, ул. акад. Г. Бончев, Бл 11, София-1113, България

Постъпила на 10 ноември 2016 г.; приета на 3 януари 2017 г.

(Резюме)

Наноразмерният $MnFe_2O_4$ има важни приложения в устройства за магнитен запис, ферофлуиди, биосензори, катализатори, направляван транспорт на лекарства в организма и др. В работата се изучават възможностите за получаване на наноразмерни $MnFe_2O_4$ по метода на синтез чрез изгаряне от разтвор. Изучени са две системи със смесени горива в различни съотношения, а именно глицин-глицерол и захароза-урея. Получените продукти са подложени на термична обработка при различни температури и в различни среди (въздух, аргон), за да се намерят оптималните условия за получаване на монофазен наноразмерен $MnFe_2O_4$. Образците са изследвани с методите на рентгеновата дифракция, нискотемпературна адсорбция на азот (БЕТ), фотоелектронна и Мьосбауерова спектроскопия. Образците, получени чрез използване на чисти въглеводороди или смеси с високо съдържание на въглеводороди показват суперпарамагнитно поведение поради малкия размер на кристалите, докато тези, получени с високо съдържание на азотсъдържащи горива показват магнитно подреждане. Показано е, че по-малките частици, получени при ниски температури на термична обработка имат по-високи стойности на решетъчните напрежения. Термична обработка при високи температури води до намаляване на напреженията без значителна промяна на размера на кристалите.

***Ключови думи**: синтез чрез изгаряне от разтвор, $MnFe_2O_4$, XRD, XPS, Мьосбауерова спектроскопия.*